THE JOURNAL OF PHYSICAL CHEMISTRY B

Article

Solvation of a Spherical Cavity in Simple Liquids: Interpolating between the Limits

Jianzhong Wu

J. Phys. Chem. B, **2009**, 113 (19), 6813-6818• Publication Date (Web): 20 April 2009

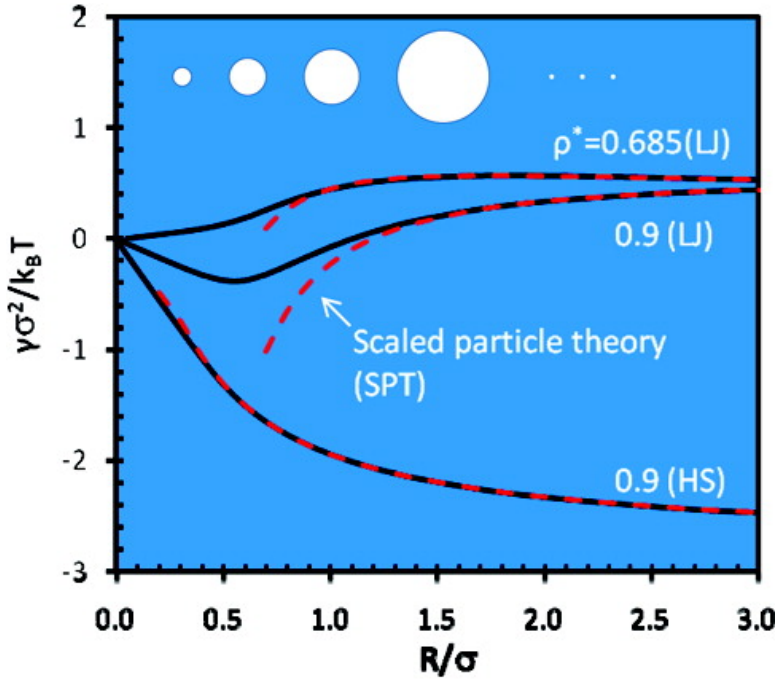

More About This Article

Additional resources and features associated with this article are available within the HTML version:

- Supporting Information
- Access to high resolution figures
- Links to articles and content related to this article
- Copyright permission to reproduce figures and/or text from this article

View the Full Text HTML

The Journal of Physical Chemistry B is published by the American Chemical Society. 1155 Sixteenth Street N.W., Washington, DC 20036

Solvation of a Spherical Cavity in Simple Liquids: Interpolating between the Limits

Jianzhong Wu*

Department of Chemical and Environmental Engineering, University of California, Riverside, California 92521

Received: February 21, 2009; Revised Manuscript Received: March 24, 2009

Dissolution of a solute molecule into a solvent necessitates the creation of a cavity devoid of solvent molecules. The cavity solvation free energy is exactly known at both very small and large length scales, but in between it can only be estimated by various approximations. Guided by simulation results for the solvation of small cavities and density functional theory, we analyze the size dependence of the solvation free energy, contact density of solvent molecules, and the interfacial tension for a spherical cavity in a Lennard-Jones fluid or a system of hard spheres. Unlike cavity formation in the hard-sphere system, a quadratic curvature expansion is insufficient to connect smoothly the exact results in the microscopic and macroscopic limits for the cavity surface tension (or equivalently, the contact solvent density) in Lennard-Jones fluids. Considering the sensitivity of solvation to molecular details at small length scales, we conjecture that, for practical purposes, a heuristic approach may be sufficient to link the thermodynamic limit at large length scales and the exact results of cavity formation at very small length scales.

I. Introduction

A central topic in solution thermodynamics, solvation has been subjected to a long history of theoretical investigations. Recent years have seen renewed interest in the statistical mechanics of solvation, primarily directed toward obtaining a better understanding of hydration and water-mediated interactions from a molecular perspective.[1] Because solvation in an aqueous solution disturbs the hydrogen-bonding network among water molecules that is difficult to be described by a semiempirical force field, a conventional statistical−mechanical method is often insufficient to quantify the solvation free energy and the local redistribution of water molecules near the solute surface.[2] Lack of precision is introduced not only by approximations of analytical methods but also, more importantly, by nonpairwise additivity of the intermolecular interactions unique for water.[3] The deficiency of classical molecular models invokes alternative approaches based either on first-principle calculations[4] or on heuristic semiempirical methods.[5,6] For practical purposes, a full quantum mechanical description of solvation awaits further improvement in computer speed and computational algorithm. Thus, it is of current interest to develop heuristic methods to describe solvation in aqueous systems.[7]

About 50 years ago, Reiss, Frisch, and Lebowitz proposed that dissolution of a solute molecule into a solvent can be considered as a two-step process: First, formation of a cavity to accommodate the solute molecule and second, application of the solute−solvent attraction.[8] The first step accounts for the molecular excluded volume effect and can be represented by dissolution of a hard body or cavity that excludes solvent molecules. The second step accounts for the attractive energy between the solute and solvent molecules and its influence on the local solvent structure. While the solvation is perceived as a two-step process, the total solvation free energy is calculated by using a semiempirical correlation near the bulk limit. The heuristic approach provides a key basis in the development of the scaled particle theory (SPT),[9] which has been successfully applied not only to hard-sphere systems, as well as documented, but also to liquid crystals[10] and hydrophobic phenomena.[7,11]

Unlike alternative methods, SPT does not require a specific molecular model for the solvent. It is appealing, in particular, for studying solvation in aqueous systems. As indicated by Reiss, Frisch, and Lebowitz,[8] the free energy or reversible work to create a spherical cavity of radius R in any solvent is related to the contact density of the solvent molecules:

$$\mathrm{W}(R) = k_{\mathrm{B}}T\int_0^R 4\pi R^2\rho(R)\,\mathrm{d}R \tag{1}$$

where k_{B} is the Boltzmann constant, T is the absolute temperature, and $\rho(R)$ is the number density of the solvent molecules at the cavity surface. Equation 1 is derived from a statistical analysis of the fluctuation of the number of solvent molecules in a spherical cavity and, thus, it is independent of specific molecular models of the solvent.

The solvent density at the cavity surface is known exactly at both small and large limits. For a small cavity that holds at most one solvent molecule, the contact density is simply related to the number density of solvent molecules in the bulk ρ_{B}:

$$\rho(R) = \rho_{\mathrm{B}}\left(1 - \frac{4}{3}\pi R^3\rho_{\mathrm{B}}\right)^{-1} \qquad R \le R_0 \tag{2}$$

where R_0 is the maximum radius such that the cavity can accommodate only one solvent molecule.

For a cavity of infinite size, the contact solvent density can be calculated from the pressure far away from the surface:

$$\lim_{R\to\infty}\rho(R) = P/(k_{\mathrm{B}}T) \tag{3}$$

Equation 3 is known as the contact value theorem. With an approximate expression for $\rho(R)$ that smoothly bridges the small and large limits, eq 1 allows us to calculate the cavity solvation free energy without using a specific molecular model for the solvent.

Because of the discreteness of the number of solvent molecules that can be accommodated in a cavity, $\rho(R)$ is not an analytical function of R. Nevertheless, it has been shown[8] that $\rho(R)$ and its first derivative are continuous at all values of

* E-mail: jwu@engr.ucr.edu.

10.1021/jp9016163 CCC: $40.75
Published on Web 04/20/2009

R. While the discontinuity in the higher order derivatives prohibits expression of $\rho(R)$ in terms of a power series of the curvature ($1/R$), Reiss, Frisch, and Lebowitz assumed that for $R_0 \leq R \leq \infty$, $\rho(R)$ can be approximated by a quadratic function of the curvature:[8]

$$\rho(R) = \rho(\infty) + a/R + b/R^2 \quad (4)$$

Because $\rho(R)$ is a smooth function in the entire range of R, the coefficients on the right side of eq 4 can be fixed by imposing the conditions of continuity for $\rho(R)$ and its first derivative at R_0, provided that the quadratic function remains valid at such small length scales.

If both the solute and solvent molecules are represented by hard spheres, eq 4, in combination with the compressibility or viral equation, leads to the SPT equation of state for hard spheres. While eq 4 appears as a truncated Maclaurin series, inclusion of higher-order terms shows virtually no improvement for determining the thermodynamic properties of hard spheres.[8] As a non-analytical function, $\rho(R)$ cannot be adequately represented by a Taylor series.

Despite the impressive success of SPT, it is not clear whether the quadratic form as given by eq 4 is sufficient to close the gap between the exact results at very small and large scales. Because of the lack of theoretical justifications, the success of SPT was sometimes considered a "mathematical miracle"[12] or "accident".[13] The approximation for the contact density is strictly valid only for large values of R and, therefore, is not relevant to that at length scales smaller than the diameter of a solvent molecule. Recently, new questions have been raised concerning the applicability of SPT to solvation of a solvophobic colloidal particle or a macromolecule that exhibits partial drying at the surface.[13−16] In particular, Evans and co-workers indicated that for cavity formation in a solvent near the vapor−liquid coexistence, neither the cavity fluid surface tension nor the solvent contact density can be expressed in terms of a power law expansion of the curvature.[13−16]

The purpose of this work is to investigate how $\rho(R)$ varies from R_0 to ∞ without using the quadratic "ansatz" or a power series expansion. To make the system viable for a quantitative analysis, we restrict our interest to solvation of a spherical cavity in a simple liquid, i.e., the solvent molecules are argon-like and the intermolecular interaction can be described by a truncated and shifted Lennard-Jones (LJ) potential. Whereas the argon-like solvent may have little similarity to liquid water in terms of microscopic details, a theoretical analysis of cavity solvation in the simple solvent may provide insights for development of an improved theory for aqueous systems. Indeed, relevance of the simple liquid model is easily seen because eqs. 1−3 are equally applicable to any solvation including water. Within the simple solvent model, we have shown in a previous work[17] that the solvent density at the cavity surface can be reliably predicted by using a density functional theory (DFT). With the knowledge of the contact solvent density in the full range of cavity size, we can calculate the solvation free energy and the interfacial tension at both small and large length scales.

II. Molecular Model and Theory

Using the LJ model for an argon-like solvent, we are interested to find the distribution of solvent molecules around a spherical cavity of radius R at fixed temperature T and bulk density ρ_B. For comparison and as a reference, we consider also cavity formation in a system of hard spheres.

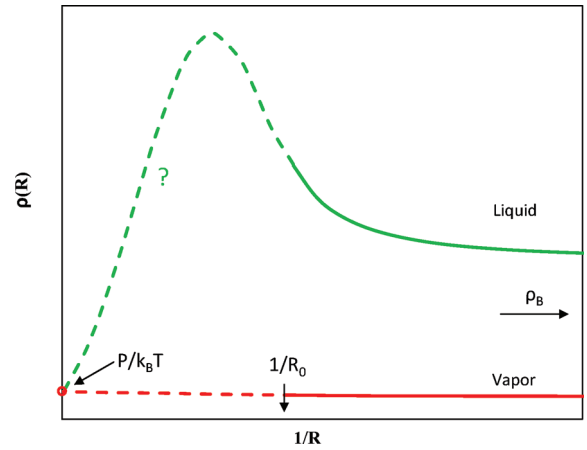

Figure 1. Schematic representation of the solvent density at the surface of a spherical cavity of radius R. The solid lines are exact results for small cavities $R < R_0$ (R_0 is the maximum radius such that the cavity can accommodate at the most one solvent molecule) and the point stands for the contact density near a cavity of infinite size $R = \infty$. The contact density depends on the cavity location if the solvent is at the vapor−liquid coexistence, i.e., the contact density on the liquid side (top) is different from that on the vapor side (bottom).

The intermolecular interaction between two argon-like molecules is described by a pairwise additive potential truncated and shifted at a cutoff distance:

$$u(r) = \begin{cases} u^{LJ}(r) - u^{LJ}(r_c), & r \leq r_c = 2.5\sigma \\ 0, & r > r_c \end{cases} \quad (5)$$

where

$$u^{LJ}(r) = 4\varepsilon\left[\left(\frac{\sigma}{r}\right)^{12} - \left(\frac{\sigma}{r}\right)^{6}\right] \quad (6)$$

In eqs 5 and 6, r represents the center-to-center distance and σ and ε are, respectively, the size and energy parameters of the LJ potential. As shown schematically in Figure 1, the contact density of the solvent is known exactly at small and infinitely large values of R (see eqs 2 and 3). The main task is to determine $\rho(R)$ between the small and large limits.

When the cavity size is comparable to that of a solvent molecule, the solvent density at the cavity surface can be readily calculated via molecular simulations.[18] However, the task becomes more demanding as the cavity size increases, in particular when a drying layer is developed as the solvent is close to the liquid side of the vapor−liquid consistence.[19] In this work, we obtain the contact solvent density by using DFT.[20] It has been shown in an earlier work[17] that DFT provides an accurate description of the distribution of the LJ particles near a hard wall or around hard spheres of different sizes. Unlike molecular simulations, DFT can be used to describe the local distribution of solvent molecules near a cavity of arbitrary size.

DFT has been previously applied to LJ fluids for studying solvation of colloidal particles,[19,21] nucleation and bubble formation,[22,23] crystal growth,[24] and surface tension.[25] Because different approximations are introduced in formulation of the free-energy functional, not all versions of DFT give the same results. For DFT used in this work, we separate the intermolecular potential into three distinct contributions: a short-range repulsion $u^{rep}(r)$, a longer-ranged attraction $u^{att}(r)$, and a truncated and shifted tail potential $u^{tail}(r)$

$$u^{\mathrm{rep}}(r)=\begin{cases}u^{\mathrm{LJ}}(r), & r\le\sigma\\ 0, & r>\sigma\end{cases} \tag{7}$$

$$u^{\mathrm{att}}(r)=\begin{cases}0, & r<\sigma\\ u^{\mathrm{LJ}}(r), & r\ge\sigma\end{cases} \tag{8}$$

$$u^{\mathrm{tail}}(r)=\begin{cases}-u^{\mathrm{LJ}}(r_c), & r<r_c\\ -u^{\mathrm{LJ}}(r), & r\ge r_c\end{cases} \tag{9}$$

As in Barker−Henderson perturbation theory,[26] the Helmholtz energy due to the short-range repulsion is approximated by that of a hard-sphere system of the same number density and effective diameter:

$$d=\frac{1+0.2977T^*}{1+0.33163T^*+0.00104771T^{*2}}\sigma \tag{10}$$

where $T^* = k_BT/\varepsilon$. The excess Helmholtz energy [i.e., the difference between the Helmholtz energy of the real system and that of an ideal gas at the same temperature and density distribution $\rho(\mathbf{r})$] for the hard-sphere system is calculated from the modified fundamental measure theory (FMT):[27,28]

$$\beta F^{\mathrm{rep}}=\int -n_0\ln(1-n_3)+\frac{n_1n_2-\mathbf{n_{V1}}\mathbf{n_{V2}}}{1-n_3}+\frac{1}{36\pi}\left[n_3\ln(1-n_3)+\frac{n_3^2}{(1-n_3)^2}\right]\frac{(n_2^3-3n_2\mathbf{n_{V2}}\mathbf{n_{V2}})}{n_3^3}\,\mathrm{d}\mathbf{r} \tag{11}$$

where $\beta = 1/(k_BT)$ and $n_\alpha(\mathbf{r})$, $\alpha = 0,1,2,3,V1,V2$, are weighted densities related to the geometry of a spherical particle and to the local distribution of the solvent molecules $\rho(\mathbf{r})$.[29] The exact expressions for the weighted densities can be found in earlier work.[27−29]

With the hard-sphere system as a reference, the excess Helmholtz energy due to intermolecular attraction is obtained from a quadratic functional expansion:[17]

$$F^{\mathrm{att}}=F^{\mathrm{att}}(\rho_B)+\mu_B^{\mathrm{att}}\int \mathrm{d}\mathbf{r}\Delta\rho(\mathbf{r})-\frac{k_BT}{2}\int\int \mathrm{d}\mathbf{r}\,\mathrm{d}\mathbf{r}'c_B^{\mathrm{att}}(|\mathbf{r}-\mathbf{r}'|)\Delta\rho(\mathbf{r})\Delta\rho(\mathbf{r}') \tag{12}$$

where $F^{\mathrm{att}}(\rho_B)$ and $c_B^{\mathrm{att}}(r)$ are, respectively, the attractive contributions to the excess Helmholtz energy and the direct correlation function of the LJ fluid at the system bulk density and temperature, μ_B^{att} is the attractive part of the excess chemical potential for the corresponding uniform fluid, and $\Delta\rho(\mathbf{r}) = \rho(\mathbf{r}) - \rho_B$. Analytical expressions for $F^{\mathrm{att}}(\rho_B)$, $c_B^{\mathrm{att}}(r)$, and μ_B^{att} have been derived by Tang using the first-order mean spherical approximation (FMSA).[30]

In eq 12, the quadratic density expansion is applied only to the attractive part of the excess Helmholtz energy. As a result, DFT is not equivalent to the hypernetted chain approximation (HNC) that uses a quadratic expansion for both attraction and repulsion. If the direct correlation function $c_B^{\mathrm{att}}(r)$ is replaced by its asymptotic expression $-u^{\mathrm{att}}(r)/k_BT$, then eq 12 would reduce to the Helmholtz energy according to the van der Waals-like mean field approximation. Separation of the Helmholtz energy into repulsive and attractive contributions makes DFT applicable to systems with a phase transition indicated by at least two local minima in the free energy.

Finally, the excess Helmholtz energy due to the truncated and shifted potential is described by a mean field approximation:[22]

$$F^{\mathrm{tail}}=\frac{1}{2}\int\int \mathrm{d}\mathbf{r}\,\mathrm{d}\mathbf{r}'u^{\mathrm{tail}}(|\mathbf{r}-\mathbf{r}'|)H(|\mathbf{r}-\mathbf{r}'|-d)\rho(\mathbf{r})\rho(\mathbf{r}') \tag{13}$$

where $H(r)$ stands for the Heaviside function, accounting for nonoverlapping of the solvent molecules. The mean field approximation is adequate for the tail potential because it becomes significant only at large intermolecular separations.

Given the analytical expressions for various contributions to the excess Helmholtz energy (eqs 11−13), we can calculate the density distribution of the solvent molecules around a cavity from the Euler−Lagrange equation:

$$\rho(r)=\rho_B\exp\{\beta\mu_B^{\mathrm{ex}}-\delta\beta[F^{\mathrm{rep}}+F^{\mathrm{att}}+F^{\mathrm{tail}}]/\delta\rho(r)-\beta\phi(r)\} \tag{14}$$

where r is the radial distance from the cavity center, μ_B^{ex} is the bulk excess chemical potential, and $\varphi(r)$ represents a one-body external potential that excludes solvent molecules from the cavity:

$$\phi(r)=\begin{cases}\infty, & r<R\\ 0, & r\ge R\end{cases} \tag{15}$$

Equation 14 is solved numerically by the Picard iterative method with a step length of 0.02σ. The solvent density at the cavity surface is readily obtained from $\rho(r)|_{r=R}$.

III. Results and Discussion

Unlike molecular simulations, the numerical performance of DFT relies on the formulation of an approximate intrinsic Helmholtz energy functional. Different formulations may lead to drastically different and sometimes even contradictory results. To ensure that DFT used in this work is reliable, Figure 2 compares DFT predictions with Monte Carlo (MC) simulation results by Ashbough (MC-A)[31] and by Huang and Chandler (MC-HC)[18] for the solvent contact density of a LJ fluid near a cavity at $T^* \equiv k_BT/\varepsilon = 0.85$ and $\rho_B^* \equiv \rho_B\sigma^3 = 0.7$. Here the dashed line represents the exact results from eq 2 at the limit of a very small cavity, and the result at $\sigma/R = 0$ is calculated

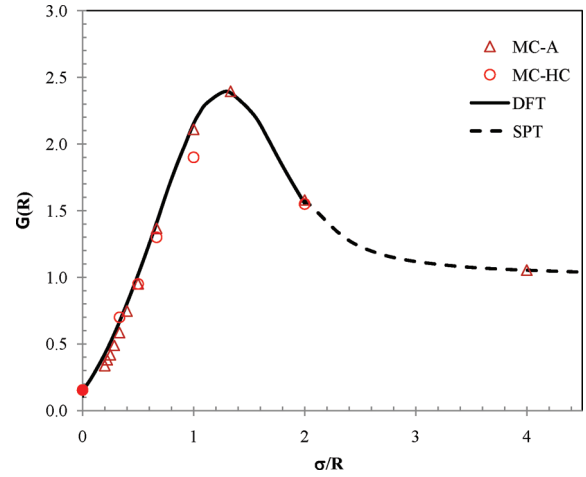

Figure 2. Comparison of theoretical predictions (DFT) with simulation results (MC) for the contact solvent density of a spherical cavity in a LJ fluid. Here $G(R) \equiv \rho(R)/\rho_B$, the dashed line shows exact results for small cavities, and the filled point is from the contact value theorem. The triangles are simulation data from MC-A, and points are from MC-HC. The LJ potential is spherically truncated and shifted at a cutoff radius $r_c = 2.5\sigma$. The temperature and density of the solvent in the bulk are $T^* = 0.85$ and $\rho_B^* = 0.7$.

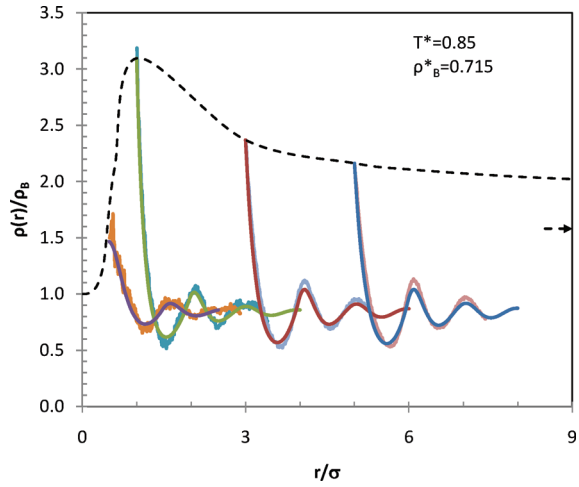

Figure 3. DFT predictions (smooth curves) and simulation results (fuzzy curves) for the density profiles of LJ particles near a cavity of radius $R/\sigma = 0.5$, 1, 3, and 5 (from left to right). The dashed line shows the contact density versus the cavity radius predicted by DFT, and the arrow on the right indicates the contact density for a cavity of infinite radius.

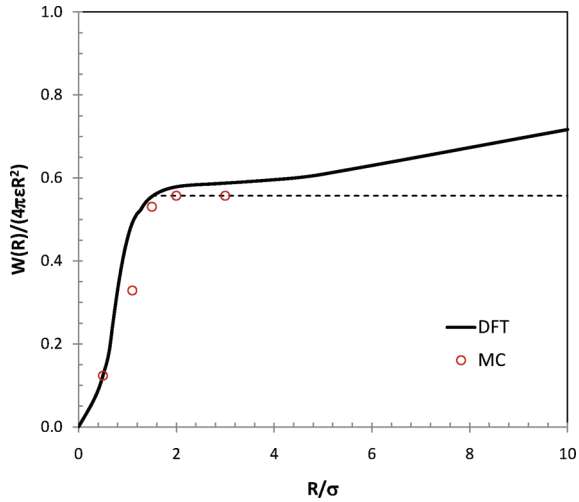

Figure 4. Solvation free energy per surface area for a spherical cavity in a LJ liquid at $T^* = 0.85$ and $\rho_B^* = 0.7$. The solid line is from DFT, and the points are from MC simulations. The thin dashed line shows a plateau suggested by MC.

from eq 3 with the reduced bulk pressure $P^* \equiv P\sigma^3/\varepsilon = 0.104$ predicted from FMSA.[30] Numerical agreement of DFT with simulation is excellent. In particular, DFT smoothly connects the exact results for a small cavity ($\sigma/R \geq 2$) and the contact density at the large cavity limit ($\sigma/R = 0$).

Figure 3 shows a further comparison of DFT results with MC simulation for the density profiles of the LJ fluid at the same temperature, but a slightly higher bulk density. Here the simulation results are generated by using a grand canonical MC simulation for over 2000 particles with a hard sphere fixed at the center of the simulation box. DFT predictions reproduce the simulation results not only for the contact density but also for the entire density profiles around hard spheres of different diameters. Good agreement was also observed upon comparison of the theoretical results with simulation for the density profiles of the LJ fluid near spherical cavities.[17]

Figure 4 shows the cavity solvation free energy predicted by DFT and MC simulations.[18] While in DFT calculations the solvation free energy is obtained by numerical integration of eq 1, the simulation results are extrapolated from the zero-occupancy limit of the probability distribution function for the number of solvent molecules within a spherical volume. Unlike the contact density, a more sophisticated simulation method must be used to compute the cavity solvation free energy; numerical uncertainty increases with cavity size. While some discrepancy is noticeable for the solvation free energy, overall the numerical agreement between DFT and simulation is satisfactory. Because creation of a cavity includes a contribution due to the volumetric work, the solvation free energy per unit area does not reach a plateau in the limit of the large cavity. Nevertheless, the simulation results appear to suggest that within a particular range of cavity size, the cavity solvation free energy is proportional to the volume at small R and the surface area at large R.

Following classical thermodynamics, we can formally divide the reversible work to form a cavity into a volumetric term that depends on the bulk pressure and a surface free energy for the creation of the interface. Toward that end, the solvation free energy can be expressed as:

$$W(R) = \frac{4\pi R^3}{3}P + 4\pi R^2\gamma \tag{16}$$

Equation 16 can be understood as a definition of the surface tension γ for the cavity−fluid interface. Because of the curvature effect, γ depends not only on temperature and pressure of the bulk fluid but also on the cavity size. With the SPT approximation for the contact density (eq 4), it is straightforward to show that the surface tension can be expressed as

$$\gamma(R) = \gamma_\infty(1 - 2\delta_T/R + \kappa/R^2) \tag{17}$$

where δ_T and κ are related to the coefficients in eq 4.[11,13]

The effect of curvature on the surface tension was known before the inception of SPT. Historically, δ_T is called Tolman length and is introduced as a first-order curvature correction of the surface tension. Equation 17 is also equivalent to a phenomenological surface free energy first introduced by Helfrich for membranes.[32] In the context of membrane mechanics, the linear and quadratic terms on the right side of eq 7 have been given physical significances, such as bending modulus or rigidity.[33] Recently, the quadratic representation of the free energy for a spherical interface has been generalized to that for interfaces of arbitrary geometry, and the phenomenological approach is entitled "morphometric thermodynamics".[34] Regardless of nomenclature, the second-order curvature correction of the surface tension is strictly valid only when the surface is near the planar limit.

From eqs 1 and 16, we can calculate $\gamma(R)$ using $\rho(R)$ as input and then check the performance of the SPT approximation in the entire range of R. Figure 5 shows the reduced cavity contact density, $G(R) \equiv \rho(R)/\rho_B$, for two LJ liquids, one at the liquid−vapor coexistence ($T^* = 0.85$, $\rho_B^* = 0.685$) and the other at the same temperature but higher density ($T^* = 0.85$, $\rho_B^* = 0.9$). The saturation density of the liquid was calculated from the FMSA.[30] For the saturated liquid, DFT calculation was stopped at $R = 100\sigma$. At $R = 100\sigma$, the contact density of the solvent molecules is $\rho^* = 0.05$, very close to that corresponding to a cavity of infinite size, $\rho^*(\infty) = 0.03$. Because $\rho(R)$ varies smoothly to the limiting value, we conjecture that for $0 < \sigma/R < 0.01$, $\rho(R)$ can be safely obtained by a simple polynomial interpolation. Figure 5 also shows the reduced contact solvent density for a cavity immersed in hard spheres with the same diameter σ. For the hard-sphere system, $\rho(R)$ is calculated from the modified FMT.[28] For both hard-sphere and LJ fluids, DFT is able to link smoothly the exact result for $R \leq \sigma/2$ and the wall density at $R = \infty$.

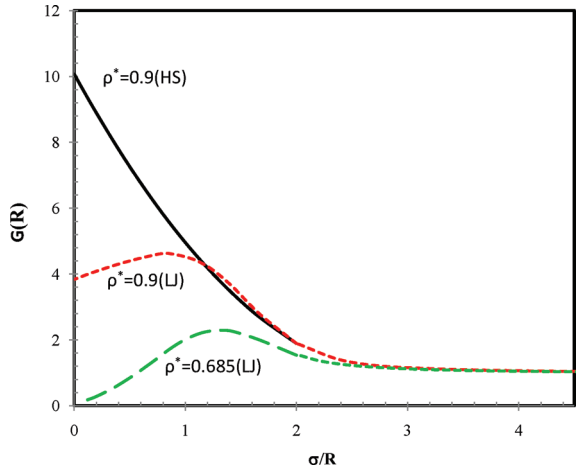

Figure 5. DFT predictions for the reduced contact density $G(R) \equiv \rho(R)/\rho_B$ for a spherical cavity of radius R in a hard-sphere fluid $\rho_B^* = 0.9$ and in LJ liquids at $T^* = 0.85$, $\rho_B^* = 0.685$ and at $T^* = 0.85$, $\rho_B^* = 0.9$.

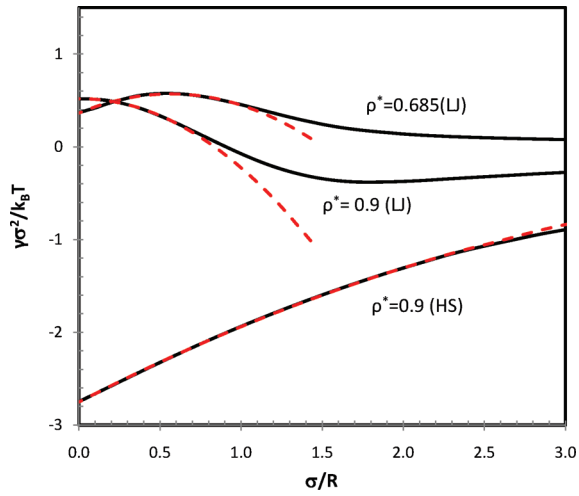

Figure 6. Cavity surface tension in the hard-sphere fluid and LJ fluids at conditions the same as those used in Figure 5. The dashed lines show correlations of the cavity surface tension with the SPT "ansatz" (eq 17).

Figure 6 presents the cavity surface tension in a LJ liquid and in a hard-sphere system. For numerical integration, $G(R)$ was fitted with a fifth-order polynomial within $0 \le \sigma/R \le 2$ for the LJ fluids and a second-order polynomial for hard spheres within the same range of R. The perfect fit of $G(R)$ with a second-oder polynomial fit affirms that the SPT approximation is adequate for the contact density of a cavity in the hard-sphere system. For the saturated LJ liquid ($T^* = 0.85$, $\rho_B^* = 0.685$), the interfacial tension exhibits a maximum, which is expected from eq 17. The maximum shifts toward the smaller curvature as density increases. For $\rho_B^* = 0.9$, the surface tension shows a minimum around $R = \sigma/2$. In contrast to that in a LJ fluid, the cavity surface tension is always negative in the hard-sphere system, and its magnitude declines monotonically with curvature.

Similar to the contact solvent density $\rho(R)$, the cavity surface tension $\gamma(R)$ is not an analytical function. Nevertheless, both are smooth functions in the entire range of R. As in the SPT approximation, $\gamma(R)$ can always be fitted into a quadratic form when the surface is sufficiently close to the planar limit. Figure 6 shows that, surprisingly, the quadratic assumption (dashed lines) is successful even when the cavity radius is comparable to the molecular diameter ($R \ge \sim 2\sigma$ the LJ fluids). In particular, the quadratic assumption reproduces the cavity surface tension up to $R = \sigma/2$ in the hard-sphere system. The excellent performance of the quadratic curvature equation at small R provides further support to the robustness of SPT approximation for hard-sphere systems. Notwithstanding this success, Figure 6 indicates that for the LJ systems, the quadratic equation for $\rho(R)$ or $\gamma(R)$ is insufficient to connect the solvation free energy at both small and large limits. In particular, the exact results for $R \le \sigma/2$ are essentially irrelevant to the quadratic form obtained from a large R. The disconnect of the SPT approximation for the surface tension at the small and large limits makes it difficult to extend the approximation to non-hard-body systems.

It has been shown that for $R > \sigma/2$, $\rho(R)$ can be related to the pair and multibody correlation functions of the solvent.[12] While a better understanding of the solvent correlation functions will help to close the gap between the microscopic and macroscopic descriptions, $\rho(R)$ is difficult to obtain even slightly beyond $R = \sigma/2$, provided that the pair correlation function of the solvent is available.[11] Because the number of solvent molecules that can be fitted into a spherical cavity rises quickly with the radius, computation of the contact solvent density requires multibody correlation functions even for a cavity comparable to the size of a solvent molecule. For aqueous systems, computer simulation or analytical prediction of the solvent structure at a small length scale is notoriously sensitive to the specifics of molecular models. In light of such difficulties, we expect that an empirical or heuristic approach may provide an effective way to close the gap between the microscopic and macroscopic limits. The "top-down" approach was recently proposed by Ashbaugh and Pratt for the development of an improved theory of hydrophobic phenomena.[7] Progress in this direction may have an impact on the modeling of biological systems with a variety of solvents.

IV. Conclusions

We have calculated the solvent contact density for a spherical cavity immersed in Lennard-Jones (LJ) liquids or in a system of hard spheres by using density functional theory (DFT). DFT predictions are in excellent agreement with simulation results from the literature. DFT calculations enable us to connect the exact results at the microscopic and macroscopic limits. Such connection was not previously examined. We find that a quadratic curvature expansion of the surface tension or, equivalently, the contact solvent density provides very good results for the hard-sphere system, but it is unable to connect the exact results at the microscopic and macroscopic limits for a LJ fluid. We have also discussed the limitation of the SPT approximations and the relevance of this work to solvation in aqueous systems. The theoretical analysis provides insights for development of a heuristic method connecting exact results for solvation at very small and large length scales.

Acknowledgment. The author wishes to dedicate this work to the 50th anniversary of the scaled particle theory (ref 8). He is indebted to Zhidong Li and Yiping Tang for generous support in numerical calculations and to John Prausnitz for editing the manuscript. He is also grateful to Henry Ashbaugh for providing unpublished simulation data, to Siegfried Dietrich for kind hospitality during his stay in Stuttgart, and to the Humboldt Foundation for financial support. Additional support for this work is from the U.S. Department of Energy (DE-FG02-06ER46296) and the National Energy Research Scientific Computing Center (NERSC).

References and Notes

(1) Chandler, D. *Nature (London)* **2005**, *437*, 640.
(2) Wu, J. Z.; Prausnitz, J. M. *Proc. Natl. Acad. Sci. U.S.A.* **2008**, *105*, 9512.
(3) Thar, J.; Reckien, W.; Kirchner, B. Car-Parrinello Molecular Dynamics Simulations and Biological Systems. In *Atomistic Approaches in Modern Biology*; Reiher, M., Ed.; Springer-Verlag: Berlin/Heidelberg, Germany, 2007; Vol 268, pp 133.
(4) Li, J. L.; Car, R.; Tang, C.; Wingreen, N. S. *Proc. Natl. Acad. Sci. U.S.A.* **2007**, *104*, 2626.
(5) Cheng, L. T.; Dzubiella, J.; McCammon, J. A.; Li, B. *J. Chem. Phys.* **2007**, *127*, 084503.
(6) Wagoner, J. A.; Baker, N. A. *Proc. Natl. Acad. Sci. U.S.A.* **2007**, *104*, 1732.
(7) Ashbaugh, H. S.; Pratt, L. R. *Rev. Mod. Phys.* **2006**, *78*, 159.
(8) Reiss, H.; Frisch, H. L.; Lebowitz, J. L. *J. Chem. Phys.* **1959**, *31*, 369.
(9) Helfand, E.; Reiss, H.; Frisch, H. L.; Lebowitz, J. L. *J. Chem. Phys.* **1960**, *33*, 1379.
(10) Cotter, M. A. *J. Chem. Phys.* **1977**, *66*, 1098.
(11) Stillinger, F. H. *J. Solution Chem.* **1973**, *2*, 141.
(12) Tully-Smith, D. M.; Reiss, H. *J. Chem. Phys.* **1970**, *53*, 4015.
(13) Henderson, J. R. *J. Chem. Phys.* **2002**, *116*, 5039.
(14) Stewart, M. C.; Evans, R. *Phys. Rev. E: Stat., Nonlinear, Soft Matter Phys.* **2005**, 71.
(15) Evans, R.; Henderson, J. R.; Roth, R. *J. Chem. Phys.* **2004**, *121*, 12074.
(16) Evans, R.; Roth, R.; Bryk, P. *Eur. Phys. Lett.* **2003**, *62*, 815.
(17) Tang, Y. P.; Wu, J. Z. *Phys. Rev. E: Stat., Nonlinear, Soft Matter Phys.* **2004**, *70*, 011201.
(18) Huang, D. M.; Chandler, D. *Phys. Rev. E: Stat., Nonlinear, Soft Matter Phys.* **2000**, *61*, 1501.
(19) Stewart, M. C.; Evans, R. *Phys. Rev. E: Stat., Nonlinear, Soft Matter Phys.* **2005**, *71*, 011602.
(20) Wu, J. Z.; Li, Z. D. *Annu. Rev. Phys. Chem.* **2007**, *58*, 85.
(21) Henderson, D.; Sokolowski, S.; Patrykiejew, A. *Mol. Phys.* **1995**, *85*, 745.
(22) Li, Z. D.; Wu, J. Z. *Ind. Eng. Chem. Res.* **2008**, *47*, 4988.
(23) Shen, V. K.; Debenedetti, P. G. *J. Chem. Phys.* **2001**, *114*, 4149.
(24) Shen, Y. C.; Oxtoby, D. W. *J. Chem. Phys.* **1996**, *104*, 4233.
(25) He, Y. J.; Mi, J. G.; Zhong, C. L. *J. Phys. Chem. B* **2008**, *112*, 7251.
(26) Barker, J. A.; Henderson, D. *J. Chem. Phys.* **1967**, *47*, 2856.
(27) Roth, R.; Evans, R.; Lang, A.; Kahl, G. *J. Phys.: Condens. Matter* **2002**, *14*, 12063.
(28) Yu, Y. X.; Wu, J. Z. *J. Chem. Phys.* **2002**, *117*, 10156.
(29) Rosenfeld, Y. *Phys. Rev. Lett.* **1989**, *63*, 980.
(30) Tang, Y. P.; Lu, B. C. Y. *AIChE J.* **1997**, *43*, 2215.
(31) Ashbaugh, H. S. , *J. Chem. Phys.* **2009**, submitted.
(32) Helfrich, W. *Z. Naturforsch., C: J. Biosci.* **1973**, *28C*, 693.
(33) Safran, S. A. *Statistical Thermodynamics of Surfaces, Interfaces, and Membranes;* Westview Press: Boulder, CO, 1994; Frontiers in Physics, Vol 90.
(34) Konig, P. M.; Roth, R.; Mecke, K. R. *Phys. Rev. Lett.* **2004**, *93*, 160601.

JP9016163